Both released silver ions and particulate Ag contribute to the toxicity of AgNPs to earthworm Eisenia fetida

Li, L.; Wu, H.; Peijnenburg, W.J.G.M.; Gestel, C.A.M. van

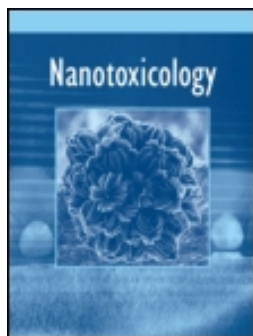# Both released silver ions and particulate Ag contribute to the toxicity of AgNPs to earthworm Eisenia fetida

Lianzhen Li, Huifeng Wu, Willie J. G. M. Peijnenburg & Cornelis A. M. van Gestel

Nanotoxicology

informa healthcare

ORIGINAL ARTICLE

Both released silver ions and particulate Ag contribute to the toxicity of AgNPs to earthworm *Eisenia fetida*

Lianzhen Li[1,2], Huifeng Wu[1,2], Willie J. G. M. Peijnenburg[3,4], and Cornelis A. M. van Gestel[5]

[1]Key Laboratory of Coastal Zone Environmental Processes and Ecological Remediation, Yantai Institute of Coastal Zone Research (YIC), Chinese Academy of Sciences (CAS), [2]Shandong Provincial Key Laboratory of Coastal Zone Environmental Processes, YICCAS, Yantai, Shandong, People's Republic of China, [3]National Institute of Public Health and the Environment, Center for Safety of Substances and Products, Bilthoven, The Netherlands, [4]Institute of Environmental Sciences (CML), Leiden University, Leiden, The Netherlands, and [5]Department of Ecological Science, Faculty of Earth and Life Sciences, VU University, Amsterdam, The Netherlands

Abstract

To disentangle the contribution of ionic and nanoparticulate Ag to the overall toxicity to the earthworm *Eisenia fetida*, a semi-permeable membrane strategy was used to separate Ag^+ released from silver nanoparticles (AgNPs) in an aqueous exposure. Internal Ag fractionation, activities of antioxidant enzymes and metabolites in *E. fetida* were determined after 96 h of exposure to two sizes of polyvinylpyrrolidone-coated AgNPs. The response of the antioxidant system combined with the content of malondialdehyde indicated that the Ag^+ released from AgNPs induced significant oxidative stress to the earthworms. Ag accumulated from AgNPs was predominantly associated with the granules and cell membrane compartments, whereas dissolved Ag was localized in the cytosol-containing fraction. In both Ag^+ exposures, two intermediates in the Krebs cycle, succinate and fumarate, were significantly elevated and depleted, respectively. A similar alteration pattern was seen in groups exposed to both smaller AgNPs (S AgNP, 10 nm) and larger AgNP (L AgNP, 40 nm), indicating that these effects in *E. fetida* were induced by exposure to released Ag^+. In addition, unique metabolic responses including decreased malate and glucose levels in S AgNP-exposed earthworms could be associated with exposure to nanoparticulate silver. Increased leucine and arginine and decreased ATP and inosine levels were observed in L AgNP exposures only, which clearly demonstrated a size-specific effect of AgNPs. Collectively, this study provided strong evidence that nanosilver acts by a different mechanism than ionic silver to cause acute toxicity to *E. fetida*, but further verification under different environmental conditions is needed.

Introduction

Due to their antimicrobial properties, silver nanoparticles (AgNPs) are currently among the most commonly used commercialized nanomaterials (Luoma, 2008). They are widely produced and technologically applied in medical devices, such as food-storage containers, soaps and sanitizers, wound dressings, and fabrics (Mueller & Nowack, 2008). With an increase in AgNP manufacture and use, it is likely that AgNPs will be released to the aquatic ecosystem, as well as deposited in soil or accumulated in sewage sludge that may subsequently be applied to soil (Chae et al., 2009). The use of sewage sludge could contribute to an input of $1 \mu g \, kg^{-1}$ of AgNPs to agricultural land per year (Mueller & Nowack, 2008). Once entered into the soil environment, AgNPs may release Ag^+ as the result of oxidation and dissolution. Approximately 10–17% of AgNPs (30–50 nm) in soils were found

to be transformed to Ag^+ after 28 d (Shoults-Wilson et al., 2011a). The dissolution of AgNPs has been shown to vary with soil composition and it is concluded that the dissolved Ag tended to bind to organic matter or clay present in soils (Cornelis et al., 2010). Thus, it is to be expected, if only because of the high concentration of DOC in pore water, that the Ag^+ concentrations are very low. It is, for instance, not possible to measure Ag^+ activities with an ion selective electrode in soil pore water, indicating that Ag^+ activities are below $10^{-10} \, mol \, L^{-1}$.

AgNPs have emerged as a topic of environmental concern as they could have unintended detrimental ecological impacts, due to their effective biocidal properties. Research regarding the potential mechanisms of toxicity of AgNPs is still emerging, with most of the available data involving freshwater species (Kennedy et al., 2010; Laban et al., 2010; Scanlan et al., 2013; Yang et al., 2012), prokaryotic and eukaryotic microorganisms (Ivask et al., 2014; Morones et al., 2005), as well as some mammalian cell lines and viruses (Cha & Myung, 2007; Kittler et al., 2010). Unfortunately, few studies have involved soil-dwelling organisms, even fewer specifically used AgNPs (Shoults-Wilson et al., 2011a,b,c; Tsyusko et al., 2012).

Hypothetical mechanisms of action of AgNPs include their penetration into cells, followed by migration to various organs and

Correspondence: Huifeng Wu, Key Laboratory of Coastal Zone Environmental Processes and Ecological Remediation, Yantai Institute of Coastal Zone Research (YIC), Chinese Academy of Sciences (CAS), Yantai, Shandong 264003, People's Republic of China. Tel: +86 535 2109190. Fax: +86 535 2109000. E-mail: hfwu@yic.ac.cn

tissues, or dissolution of the nanoparticles followed by internalization of the ionic Ag species, and subsequent induction of toxic effects (Yin et al., 2011). One study reported that cysteine, a strong Ag^+ ligand, partially alleviated AgNP toxicity to human cells (Kawata et al., 2009), while others found that AgNP cytotoxicity was independent of Ag^+ concentration and resulted primarily from oxidative stress (Eom & Choi, 2010; Kim, 2009). As an alternative, it is possible that the toxicity of AgNPs is mainly attributed to the release of soluble Ag^+. For example, no toxicity was observed when free Ag^+ was complexed by different ligands (Kim et al., 2011; Meyer et al., 2010; Miao, 2009; Xiu et al., 2011; Yang et al., 2012). Thus, to date the extent to which ionic and nanoparticulate Ag contribute to the overall toxicity of AgNPs remains an open question.

Discerning the contribution to toxicity of AgNPs versus Ag^+ ions is challenging due to their common co-occurrence. In most cases, comparative toxicity assessments of AgNPs and Ag ions were performed in parallel experiments using identical concentrations of $AgNO_3$ or supernatants of ultracentrifuged AgNP solutions to understand their different mechanisms of toxicity, regardless of the dynamic dissolution of Ag^+ from the AgNPs. This experimental setup might have a significant influence on the observed toxicity of the AgNPs. This study aims to resolve these outstanding questions about AgNP toxicity to terrestrial invertebrate earthworms, using *Eisenia fetida* as the model organism, in order to determine whether and to what extent the release of Ag^+ from the nanoparticles alone contributes to the acute toxicity of AgNPs. To provide new insights that help to understand AgNP behavior in standardized (or well-established) media previously used for metal exposure, aqueous test media instead of soil were used in this study.

For the evaluation of the potential toxicity of nanoparticles, fast and high throughput methods are needed. The omics technologies are particularly well suited to evaluate toxicity in both *in vitro* and *in vivo* systems. Metabolomics can rapidly screen for biomarkers related to predefined pathways or processes in biofluids and tissues (Jones et al., 2008; Schnackenberg et al., 2012). Specifically, little is known about the mechanisms of action of nanoparticles as these are generally difficult to measure by conventional/traditional methods. Thus, metabolomics can provide possible mechanistic insights into nanotoxicity. It has been used to study the toxic effects of a wide variety of environmental contaminants to earthworms (Brown et al., 2009; Bundy et al., 2004; Guo et al., 2009; Jones et al., 2008). Yet, few metabolomics studies have been reported for nanomaterials in earthworms, a knowledge gap that this research aims to redress.

In the present study, the toxic effects of AgNPs and their released Ag^+ ion on the earthworms *E. fetida* were assessed and compared using short-term aqueous exposures. Assessment of earthworm responses to the AgNPs was performed using ${}^1H$ NMR-based metabolomics, which seeks to identify alterations in the profile of endogenous metabolites. The observed alterations in metabolite profiles may provide insights into the molecular mechanisms of AgNP toxicity in *E. fetida*. A semi-permeable membrane strategy was used to separate the Ag^+ released from AgNPs considering the dynamic dissolution of Ag^+, thus to disentangle the contribution of exposure to Ag^+ ions and AgNPs to the overall toxicity in the aqueous exposure experiments. As a second test of nanoparticle uptake we applied a protocol as previously described (Li et al., 2011; Vijver et al., 2004), which separates tissues into operationally defined subcellular fractions with differing ecotoxicological relevance, to test if internal Ag distribution differed among treatments. In addition, the effects of nanoparticle size on toxicity were also considered by exposing the earthworms to two types of size-controlled AgNPs.

Material and methods

Synthesis and characterization of AgNPs

Two sizes (10 and 40 nm) of AgNPs were synthesized by reducing silver nitrate solution, using sodium hypophosphite and stabilized with polyvinylpyrrolidone (PVP). Details of particles synthesis, purification and storage are described in detail by Liu et al. (2009) and summarized in the Supplementary Material. The Ag concentrations of the NP solutions were measured using inductively coupled plasma-mass spectrometry (ICP-MS; Agilent 7500i, Agilent Technologies Co. Ltd, Palo Alto, CA) after digestion with 65% HNO_3.

The morphology and size of the AgNPs used were determined by transmission electron microscopy (TEM) (H-7500, Hitachi, Tokyo, Japan) at 80 kV accelerated voltage on a Philips EM420 at 120 kV and scanning electron microscopy (SEM; S-4800, Hitachi, Tokyo, Japan) coupled with energy-dispersive X-ray spectroscopy (EDS, Oxford, UK) at 15 kV. TEM samples were prepared by placing a drop of fresh AgNP suspension in water on copper grids with a continuous carbon film coating, followed by solvent evaporation at room temperature overnight. The size distribution of the nanoparticles was estimated using Image-Pro plus software (Media Cybernetics, Silver Spring, MD) and Gaussian fitting. At least 300 particles were counted from a multipicture in each case. SEM samples were prepared by loading 10 μL aliquots of the aqueous sample or the TX-114-rich phase onto a carbon supporter. The UV–VIS spectra from 300 to 700 nm were obtained using a Shimadzu UV-1700 PharmaSpec (Shimadzu, Kyoto, Japan).

AgNPs were characterized under experimental conditions for size and zeta-potential by dynamic light scattering (DLS) using a Zeta Sizer (Nano ZS, Malvern Instruments, Worcestershire, UK). Three successive measurements within an interval of 2 min were performed on two samples.

Dynamic dissolution of Ag^+ from AgNPs

In order to investigate the dynamic dissolution of Ag^+ from AgNPs under the same condition as in the earthworm exposures, a system installed for the earthworm exposure experiments (Figure S3) was used to analyze the concentration of soluble Ag released from the AgNPs, including similar time-frames. Dialysis tubes (molecular-weight cut-off of 10 kD, MWCO-10000, Shanghai Sangon Biological Engineering Technology & Services Co. Ltd, Shanghai, China) were used as a semi-permeable barrier between the two chambers. Its semi-permeability allowed for Ag^+ ions to diffuse through the membrane, while the AgNPs were held inside the dialysis tube. An AgNP exposure solution of $1 \, mg \, L^{-1}$ was diluted with sterile ultrapure water (Milli-Q, Millipore, Bedford, MA, 18.2 MΩ cm) using $1 \, g \, L^{-1}$ dispersion as stock solution and placed in one chamber, and the same volume of simulated soil solution was placed in the other chamber of the system. To avoid an uncontrolled loss of silver ions from the solution caused by precipitation as AgCl, we used a specially designed chloride-free simulated soil solution. The test solutions containing 0.1 mM Ca^{2+}, Mg^{2+}, K^+ and 1.0 mM Na^+ were prepared by adding different volumes of stock solutions of $Ca(NO_3)_2$, $MgSO_4$, $NaNO_3$ and KNO_3 to deionized (DI) water. These concentrations were selected on the basis of the average concentrations of major cations in pore water of soils (Sumner, 2000), and they were similar to the concentrations typically used in toxicity testing (Kiewiet & Ma, 1991; Li et al., 2011). Ion-release experiments were conducted at 25 °C in the dark and the solution was stirred gently. Dissolved silver concentrations in the systems were measured after 12 h and subsequently every 24 h using ICP-MS. All experiments were run

in duplicate, and the results presented are the average of duplicate measurements.

To ensure that no nanoparticles were present in the solutions outside the semi-permeable membrane, we performed a number of control experiments where the solutions underwent ultracentrifugation and nanofiltration to remove any AgNPs that might have escaped from the dialysis tube. In all cases, there was no difference between the silver concentrations. It can therefore be safely assumed that the detected silver concentrations are only due to silver ions and not AgNPs. SEM-EDS analysis and the absence of a detectable plasmon resonance optical absorption peak also confirmed the absence of AgNPs in the solution outside the semi-permeable membrane.

Animals and exposure study

The earthworm species *E. fetida* used in this study was supplied by the Ecotoxicology Laboratory in the Institute of Soil Science, Chinese Academy of Sciences. The earthworms were cultured in cattle manure in a climate-controlled room, in the darkness at a constant temperature of $25\,°C$, and at a moisture content of the culture substrate between 63% and 68%.

Prior to the test, mature earthworms weighing between 200 and 385 mg were taken from the cultures, rinsed with reagent grade water and placed on moist filter paper for 24 h to depurate their gut content. After adding 200 ml of ultrapure water containing $1\,mg\,L^{-1}$ AgNPs and simulated soil solution to different test chambers of the installed system (Figure S2), the test systems were allowed to equilibrate for several days. Tests were performed by exposing two earthworms in each chamber. For each size of AgNPs and each control experiment, eight replicates were included. Earthworms exposed to AgNP-free test solution were used as controls. The earthworms often showed an avoidance response when exposed to the test solutions. A lid with some small holes was employed to avoid the earthworms escaping from the containers and to prevent extensive moisture loss. The test employed semi-static exposures under the same conditions as described above with test solutions being renewed daily by transferring organisms to newly prepared exposure chambers. After 96 h of exposure, the earthworms were rinsed with reagent grade water, weighed and frozen at $-20\,°C$ for subsequent analysis.

Measurement of enzymatic activity and MDA content

After exposure, the earthworms were collected, frozen and stored separately at $-20\,°C$ for further treatment. The samples were rinsed with 0.15 mM KCl solution and homogenized on ice with 50 mM phosphate buffer (pH 7.0). The suspension was sonicated in an ultrasonic bath for 30 min and then centrifuged at $10\,000 \times g$ at $4\,°C$ for 10 min. The supernatant was then removed and stored at $-80\,°C$, prior to analysis.

Catalase (CAT) activity was measured using the Abei method, in which 50 mM H_2O_2 was used as a substrate (Abei, 1974). A solution of 50 mM peroxide was prepared in 50 mM potassium phosphate buffer. The decomposition of H_2O_2 catalyzed by CAT was followed using UV spectroscopy on the basis of the absorbance of H_2O_2 at a wavelength of 240 nm at the optimum pH for CAT activity (7.0).

Superoxide dismutase (SOD) activity was measured using an SOD assay kit (Dojindo Laboratories, Kumamoto, Japan). Total protein concentration was measured using the Bradford method, with bovine serum albumin as the standard protein (Bradford, 1976).

The contents of total protein and malondialdehyde (MDA) were determined using kits obtained from the Nanjing Jiancheng Bioengineering Institute. All the results were expressed with

reference to protein concentrations determined according to Bradford (1976).

Subcellular Ag distribution in the earthworms

In order to compare the distribution of Ag in the earthworms exposed to AgNPs or the Ag^+ released from the NPs, the differential centrifugation scheme of Vijver et al. (2006) (Figure S1) was used to produce four operationally defined subcellular fractions. More detailed subcellular fractionation procedures were supplied in Supplementary Material. Briefly, two earthworms from each treatment were washed with dilute EDTA solution and then rinsed with 400 mL of DI water three times, fast frozen in liquid nitrogen and stored at $-80\,°C$ before they were homogenized (1:10 w/v ratio) in 10 mM Tris-base buffer (pH 7.6) using a polytron homogenizer on ice. Homogenates were centrifuged using an Optima™ L-80XP Preparative Ultracentrifuge (Beckman Coulter, Fullerton, CA). A total of four different fractions associated with granules (fraction D), cell membranes (fraction E), microsomes (fraction F) and the cytosol (fraction G) were obtained.

Following fractionation, all samples were digested with 65% HNO_3 (Aristar grade, BDH Chemicals Ltd., Poole, Dorset, UK) as described for total metal analysis and Ag was determined by ICP-MS. Ag concentrations in the different fractions are expressed as µg Ag g^{-1} (fw) *E. fetida*. The distribution of Ag among the different fractions was compared with the basis of the percentage of each fraction of the total Ag content in the earthworms.

Statistical analyses

All data are reported as mean $\pm$ standard deviation (SD). Differences in Ag concentrations among the fractions of each treatment and between exposed and control earthworms were compared using a one-way analysis of variance (ANOVA), followed by a Tukey HSD *post-hoc* test. Differences were considered statistically significant at $p \leq 0.05$. All data were analyzed using SPSS (Version 10.0, Chicago, IL) statistical software (Statistical Graphics Corp., Princeton, NJ).

Results

AgNPs characterization

The AgNPs studied herein varied in their primary size but had the same surface coating of PVP. The SEM images indicated that spherical shapes of zerovalent silver, with mean size of 40 ± 10 and 10 ± 4.0 nm, respectively, for the smaller AgNPs (in the following text named S AgNP) and larger AgNPs (L AgNP) (Figure 1A and B). The SEM-EDS elemental spectrum showed the presence of Ag, chemically confirming the formation of AgNP particles. TEM analysis confirmed these results, and also revealed that the size of the L AgNP ranged from 30 to 50 nm (Figure 1C), while the S AgNP had an average size of 10 nm (Figure 1D). As shown in Figure 2, a single plasmonic resonance peak was observed at 410 nm, which was indicative of the presence of AgNPs (Mie, 1908) and the narrow peak indicated the smaller size of the particles.

When dispersed in DI water, the hydrodynamic diameter of both the nanoparticles increased compared with their primary size, but the average diameter of AgNPs remained under 60 nm (Table S1) in all cases. When the particles were dispersed in a simulated soil solution at pH 6.8, their hydrodynamic diameter increased even further, with the mean size of the agglomerated particles in the test medium being 47.4 ($\pm$3.21) nm and 68.2 ($\pm$27.5) nm for S AgNP and L AgNP, respectively (Table S1). The surface charge determined by the measurement of their zeta-potential showed that the S AgNP had a slightly more
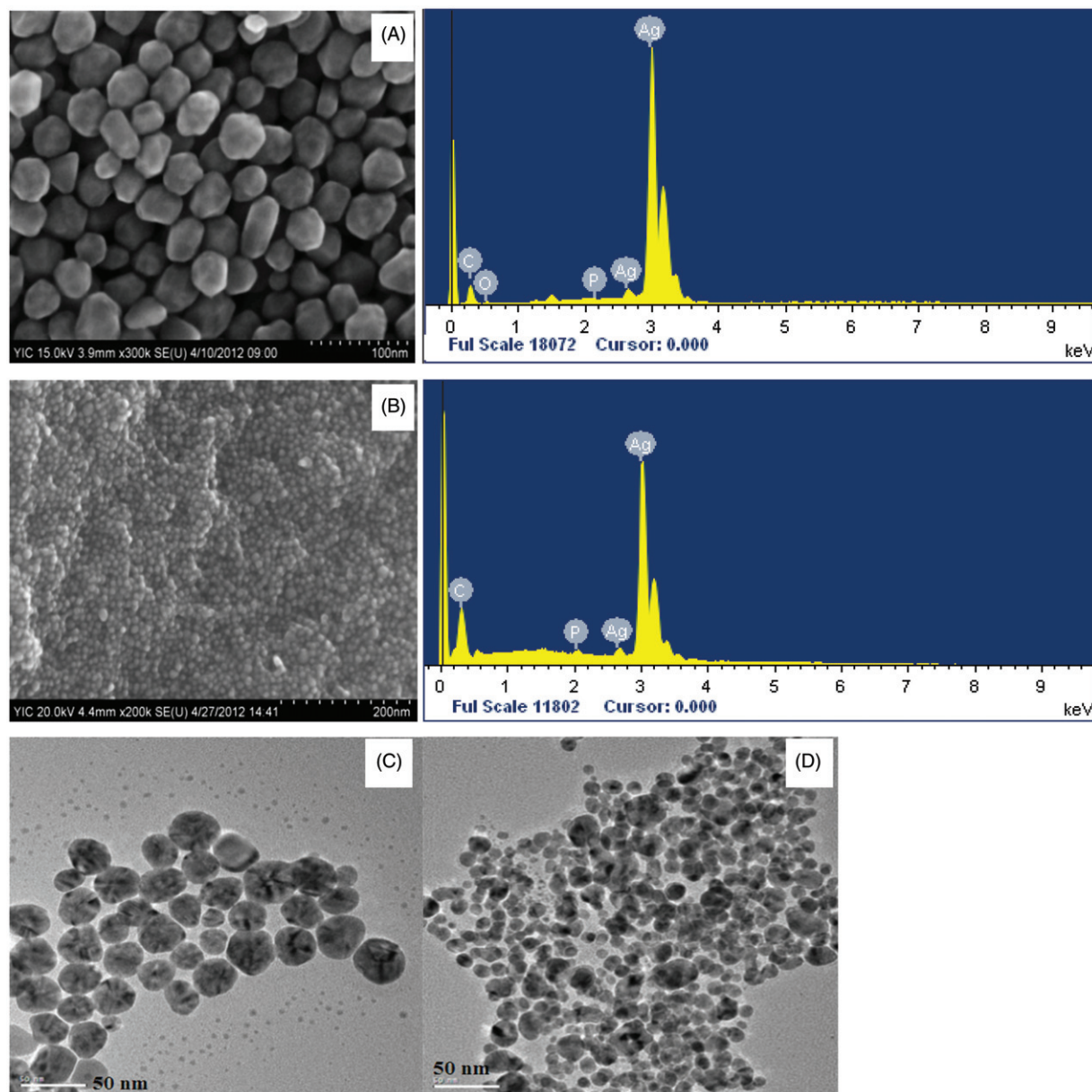
Figure 1. TEM and SEM images and energy-dispersive X-ray (EDX) of two sizes of PVP-capped AgNPs used in this study. As depicted in the SEM (A) and TEM images (C) the larger AgNPs had a size of 30–50 nm, while the SEM (B) and TEM image (D) showed that the smaller AgNPs had an average size of 10 nm, EDX analysis of Ag NPs shows the elemental Ag composition (at the right-hand side of A and B).

negative zeta-potential ζ (-15.1 ± 6.09 mV) than the L AgNP (-13.3 ± 9.89 mV; Table S1). Despite some aggregation in the simulated soil solution, the average size of the NP agglomerates remained below 100 nm under these conditions (Table S1) and remained stable for at least 96 h, which was the time period used for the toxicity studies.

Dynamic dissolution of AgNPs

The Ag^+ release of these two AgNPs was carefully studied based on dialysis experiments using ICP-MS. Figure 3 shows the dissolution curves for the two AgNPs under the same conditions as used for the earthworm exposures. Upon the addition of the stock nanoparticle suspensions, the Ag^+ concentration in the AgNP-amended suspensions averaged $1.25 \pm 0.1\,\mu g\,L^{-1}$ and $0.50 \pm 0.3\,\mu g\,L^{-1}$ for the S AgNP and L AgNP, respectively. The data indicate that the release of Ag^+ is much higher for S AgNP than for L AgNP as the concentration of dissolved Ag species increased significantly from 1.25 to $10.3\,\mu g\,L^{-1}$ over a 6 d observation period versus an increase of 0.5–$4.7\,\mu g\,L^{-1}$ (Figure 3).

Subcellular fractionation of Ag in the earthworm *E. fetida*

To investigate the effects of ionic and nanoparticulate Ag on Ag uptake and toxicity for the earthworm *E. fetida*, a semi-permeable membrane strategy was used to separate Ag^+ released from AgNPs (Figure S3). In the following text, the two groups of released Ag^+ exposures from the smaller and larger AgNPs are referred to as Ag^+ (S AgNP) and Ag^+ (L AgNP). After four days of exposure, *E. fetida* accumulated Ag in its body from the simulated soil solutions containing $1.0\,mg\,L^{-1}$ of the two sizes of AgNPs and their released Ag^+. No detectable Ag accumulation was found in the control earthworms incubated for 96 h in non-amended simulated soil solution. The whole-body concentrations of Ag in the earthworms were comparable for exposures to S AgNP and Ag^+ (S AgNP), amounting 31.0 ± 0.6 and $32.3 \pm 6.1\,\mu g\,g^{-1}$ wet weight, respectively. For L AgNP, at the end of 4-d exposures (Figure 4A), tissue concentrations of Ag were significantly ($p < 0.05$) higher in individuals exposed to AgNPs than to Ag^+ (L AgNP). In addition, after 4 d of exposure, *E. fetida* accumulated significantly higher Ag concentrations

(A)

(B)

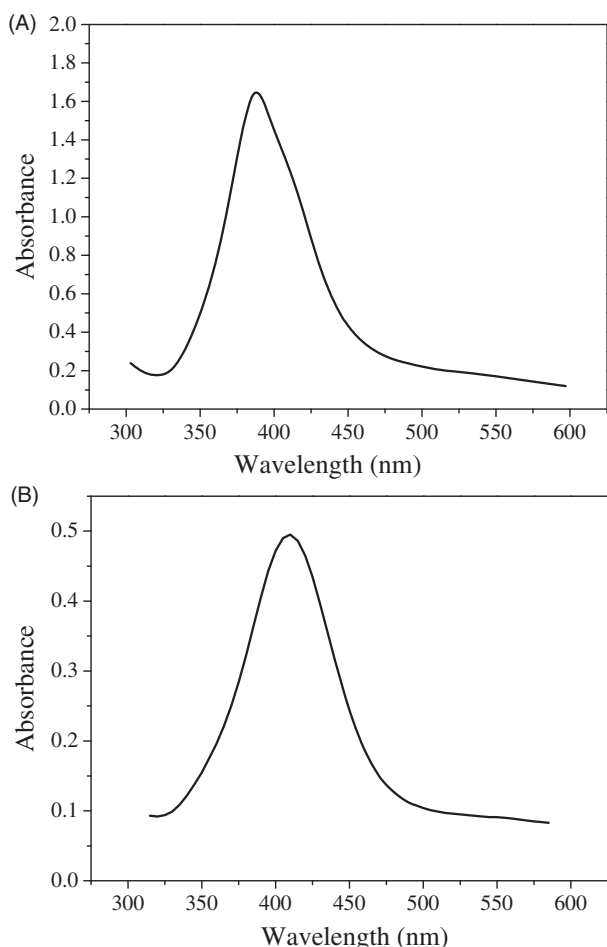Figure 2. UV–Vis absorption spectrum of the PVP-capped 10 nm (A) and 40 nm AgNPs (B) in DI water.

Figure 3. The extent of Ag$^+$ ion release from $1 \, mg \, L^{-1}$ of smaller (10 nm, S AgNP) and larger (40 nm, L AgNP) AgNPs as a function of time in a simulated soil solution at $25\,^\circ$C in the dark. Error bars represent the standard deviation of the mean of three replicates.

when exposed to the larger particles than to the smaller particles (Figure 4A), but significantly lower Ag concentrations when exposed to the Ag$^+$ (L AgNP) than to Ag$^+$ (S AgNP) (Figure 4A).

The percentage of accumulated Ag associated with different intracellular fractions, the granules and cytosol fractions from the two AgNP treatments was significantly different when compared with the corresponding released Ag$^+$ treatments (Figure 4B and C, one-way ANOVA, $p < 0.05$). In the earthworms exposed to AgNPs, more Ag was accumulated in the granules and cell membrane fractions (fractions D and E; representing 66.5% and 59.4% of the body burden for the S AgNP and L AgNP, respectively) and less in the microsome and cytosol fractions (fractions F and G; representing 33.5% and 40.6% of the body burden for the S AgNP and L AgNP, respectively). The proportion of Ag accumulated in the different fractions of the earthworms exposed to the Ag$^+$ released from AgNP was quite different, with the largest proportion of Ag (representing 43.1% and 41.5% of the body burden for the S AgNP and L AgNP, respectively) in fraction G (containing cytosol).

Antioxidant enzymatic activities and MDA content in the earthworm *E. fetida*

The activities of SOD in *E. fetida* exposed to the Ag$^+$ released from both small- and large-sized AgNPs increased significantly ($p < 0.05$) compared with the controls. On the other hand, the SOD activity in earthworms exposed to AgNPs did not differ significantly from the controls (Figure 5A). The activities of CAT in animals demonstrated similar responses as the activities of SOD, being highest in earthworms exposed to the Ag$^+$
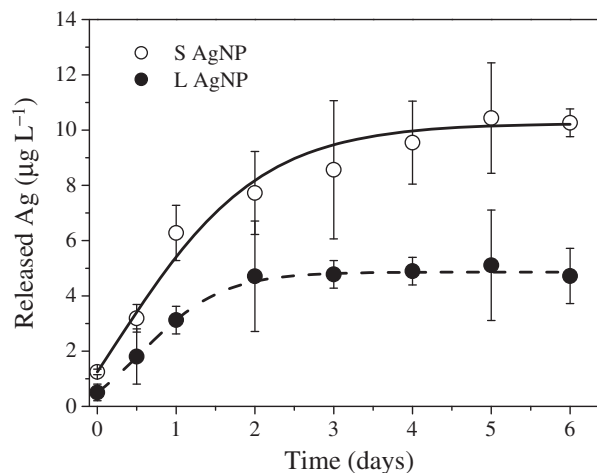
(S AgNP), compared with the control and the L AgNP treatments (Figure 5B). As described in Figure 5(C), the MDA level was similar in different treatments, which was clearly different from the profiles of SOD and CAT.

Metabolic responses in *E. fetida* exposed to AgNPs and released Ag$^+$

A representative ^{1}H NMR spectrum of earthworm extracts from the control is shown in Figure S2. Several classes of metabolites were identified, including amino acids (valine, leucine, isoleucine, alanine, arginine, glutamate, glumatine, glycine, etc.), organic acids (succinate and fumarate), organic osmolytes (betaine, myo-inositinol dimethylglycine and dimethylamine) and energy storage compounds (ATP, glucose and maltose).

Principle component analysis (PCA) was initially performed on the NMR spectral data sets from control, AgNP and released Ag$^+$ exposed groups. PCA resulted in significant ($p < 0.05$) separations between control and all exposures along different PC axes (data not shown), which implied that the AgNPs and their released Ag$^+$ induced significant metabolic responses in earthworms. In further orthogonal partial least-squares-discriminant analysis (O-PLS-DA), scores plots and corresponding loading plots for the pair-wise discrimination between control, AgNP and released Ag$^+$-exposed groups are shown in Figures 6 and 7.

The O-PLS-DA coefficients demonstrated that alanine, succinate and phosphocholine were higher in the S AgNP-exposed earthworms than in the control group, while the levels of malate, glucose and fumarate were lower than in the control group (Figure 6). For the exposure of Ag$^+$ (S AgNP), alanine, succinate, phosphocholine and fumarate levels in *E. fetida* were altered in a similar fashion (Figure 6). However, malate and glucose levels were not altered in the Ag$^+$ (S AgNP)-treated group. The levels of other metabolites, including threonine, arginine and myo-inositol, were significantly decreased in the Ag$^+$ (S AgNP)-treated group, which was different from the patterns of these metabolites in the S AgNP-treated group. Metabolic responses in *E. fetida* exposed to L AgNP included increased succinate, leucine, arginine and inosine, and decreased fumarate and ATP levels (Figure 7). In the Ag$^+$ (L AgNP) and the L AgNP-exposed earthworms, the intermediates in the Krebs cycle, succinate and fumarate, were altered in a similar way (Figure 7). The levels of three amino acids, including
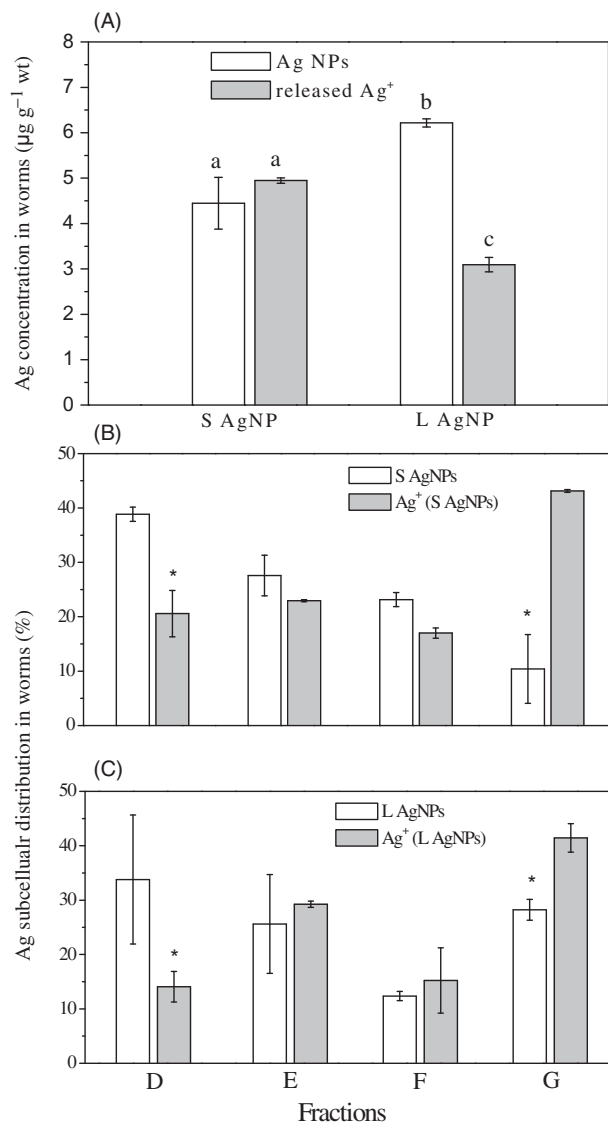
Figure 4. Total accumulation (A) and subcellular distribution of Ag (represented as the percentage of the accumulated Ag associated with different intracellular fractions; B and C, for smaller AgNP and larger AgNP, respectively) in the earthworm *E. fetida* after 4-d exposure $1 \, mg \, L^{-1}$ two sizes of PVP-capped AgNP and the corresponding released Ag^+. Values are means $\pm$ SD ($n = 3$). Bars with different letters are significantly different ($p < 0.05$) for total Ag accumulation in A. Clear bars are animals exposed to AgNPs; gray bars are animals exposed to only to released Ag^+; one asterisk denotes significant differences between AgNPs and released Ag^+-exposed earthworms for a specific fraction (*t*-test) at $p < 0.05$. Fractions D, E, F and G represent granules and cell membranes, microsomes and the cytosol, respectively.

aspartate, asparagine and phenylalanine, were significantly elevated, while glucose and maltose were depleted in the Ag^+ (L AgNP)-exposed group, which was different from the patterns of these metabolites in the L AgNP-treated group.

Discussion

DLS measurement indicated that the hydrodynamic diameter of AgNPs increased even further, when the particles were dispersed in a simulated soil solution than that in DI water. This was most likely due to the higher ionic strength of the simulated soil solution as in the case of DI, which resulted in the aggregation of nanoparticles and subsequently reduced the effective surface area, and finally limited the release of soluble Ag (He et al., 2013).
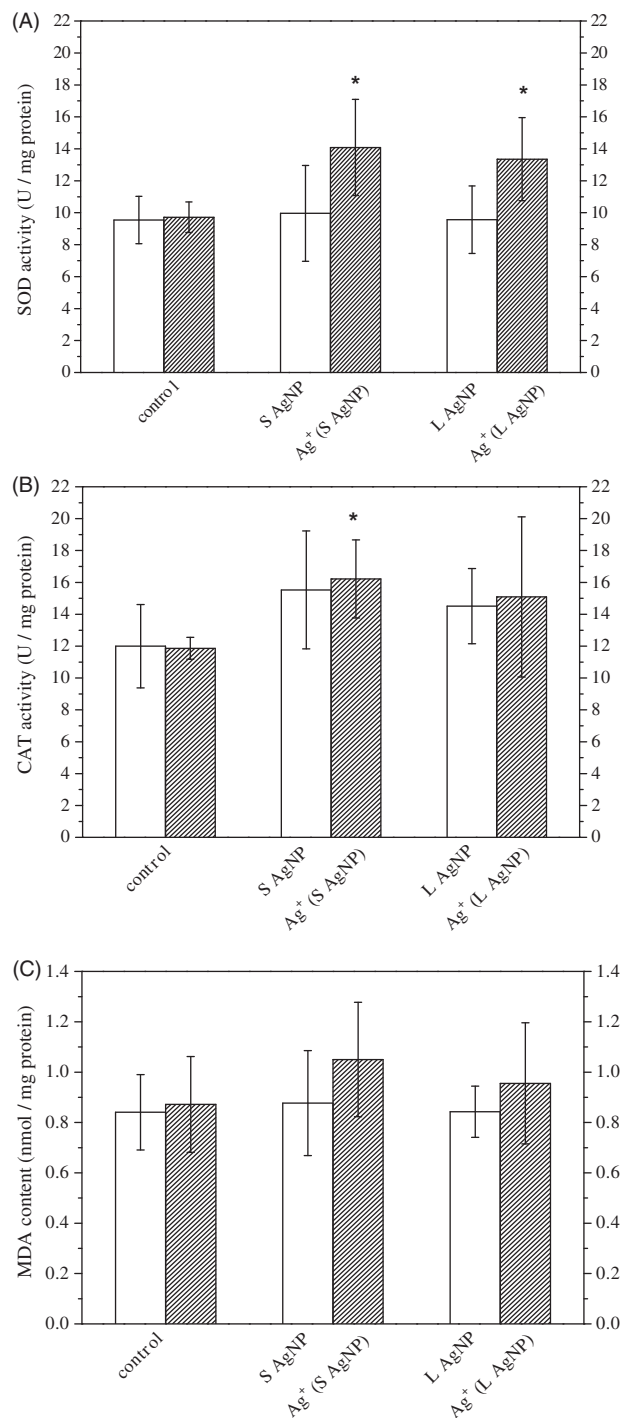

Figure 5. SOD (A), CAT (B) activities and MDA (C) content in the earthworm *E. fetida* after 96 h exposure of $1 \, mg \, L^{-1}$ two sizes of PVP-capped AgNP and the corresponding released Ag^+. The smaller AgNPs (named S AgNP) and larger AgNPs (L AgNP) had an average size of 10 and 40 nm, respectively. The two groups of released Ag^+ exposures from the small and large AgNPs are referred as Ag^+ (S AgNP) and Ag^+ (L AgNP), respectively. Error bars represent the standard deviation of the mean of three replicates. Significantly different from the control: *$p < 0.05$.

Because Ag^+ ions released upon dissolution of AgNPs have been proposed to be the primary contributor to the toxicity of AgNPs (Kim et al., 2011; Meyer et al., 2010; Miao, 2009; Xiu et al., 2011; Yang et al., 2012), we performed toxicity and dissolution tests in parallel. For the systems studied, the amount of silver released was less than 2% (2% and 1% for S AgNP and L AgNP, respectively) of the total amount of silver present in the
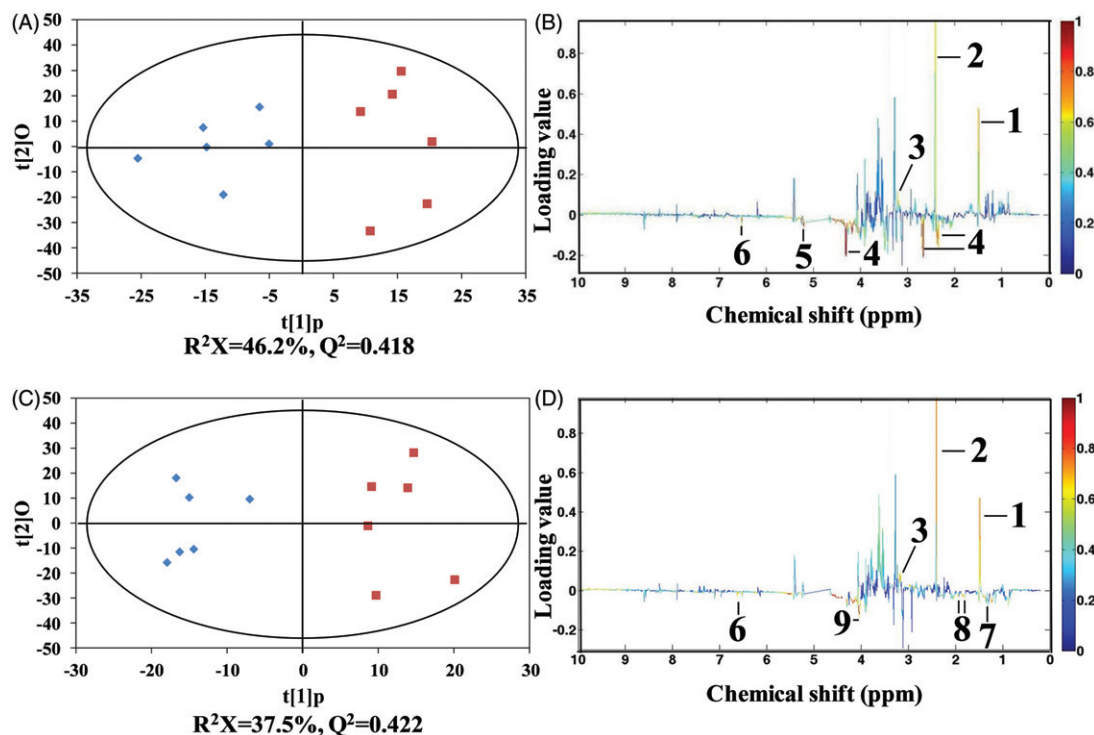
Figure 6. O-PLS-DA score plots derived from ^{1}H NMR spectra of tissue extracts from earthworms *E. fetida* exposed to controls (♦) and 1 mg L^{-1} small (10 nm) AgNPs (■) (A), and control (♦) and Ag$^+$ released from small AgNPs (■) (C) for 96 h, and corresponding coefficient plots (B) and (D). The color map shows the significance of metabolite variations between the two classes (control and treatment). Peaks in the positive direction indicate metabolites that were more abundant in the treatments, metabolites that were more abundant in the control are presented as peaks in the negative direction. Metabolites were assigned and labeled in Figure S2. Keys: (1) alanine, (2) succinate, (3) phosphocholine, (4) malate, (5) α-glucose, (6) fumarate, (7) threonine, (8) arginine and (9) myo-inositol.
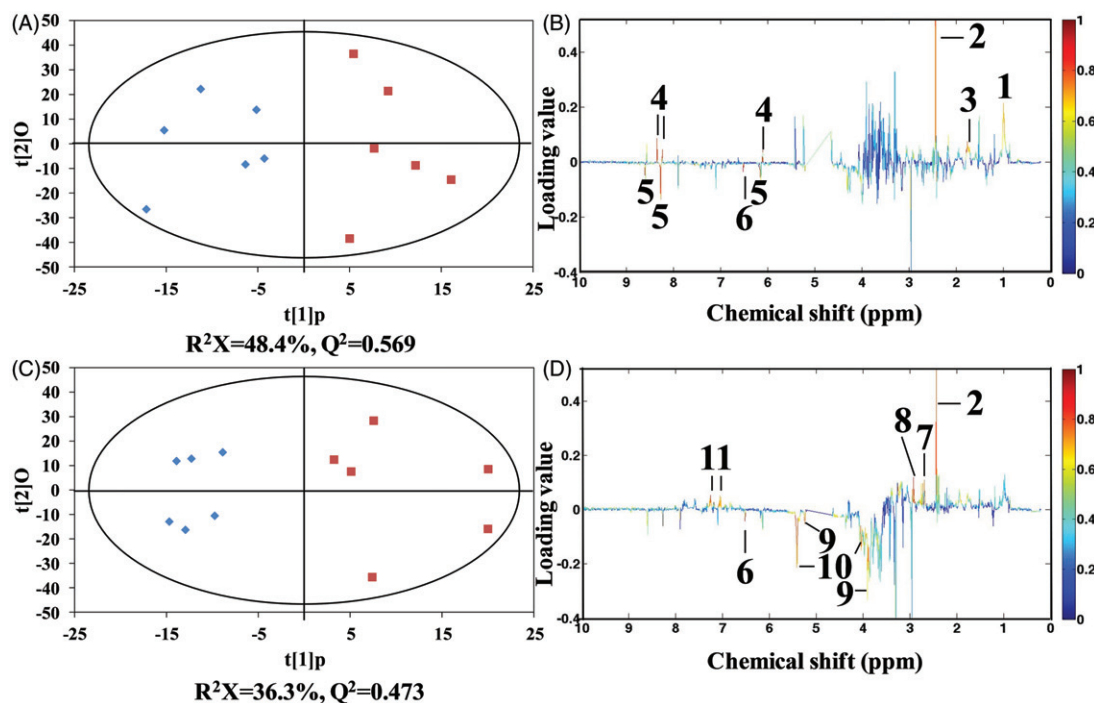

Figure 7. O-PLS-DA score plots derived from ^{1}H NMR spectra of tissue extracts from earthworm *E. fetida* exposed to control (♦) and 1 mg L^{-1} large (40 nm) silver nanoparticle treatment (■) (A), and control (♦) and the released Ag$^+$ treatment from large silver nanoparticle (■) (C) for 96 h, and corresponding coefficient plots (B) and (D). The color map shows the significance of metabolite variations between the two classes (control and treatment). Peaks in the positive direction indicate metabolites that are more abundant in the treatments. Consequently, metabolites that are more abundant in the control group are presented as peaks in the negative direction. Metabolites were assigned and labeled in Figure S2. Keys: (1) leucine, (2) succinate, (3) arginine, (4) inosine, (5) ATP, (6) fumarate, (7) aspartate, (8) asparagine, (9) α-glucose, (10) maltose and (11) phenylalanine.

systems after the addition of the nanoparticles. This differs from the complete particle dissolution observed by Liu & Hurt (2010) in air-saturated DI water. It should be noted, however, that silver concentrations of this magnitude and even lower can cause biological effects to common terrestrial and aquatic organisms (Ratte, 1999).

Differential centrifugation showed that exposure to AgNPs and the released Ag⁺ led to different intracellular partitioning patterns of Ag in the earthworms, particularly with respect to the fractions G (cytosolic fraction) and D (granules). In the earthworms exposed to the Ag⁺ released from AgNP, the largest proportion of Ag was found to be associated with fraction G (containing cytosol). In these fractions, a portion of the Ag body burden appeared to be bound to a metallothionein-like protein, which constitutes the putative detoxification mechanism (Li et al., 2011; Vijver et al., 2006). This is comparable to previous results for the Polychaete *Nereis diversicolor* (García-Alonso et al., 2011). MT is a stress protein that belongs to a super-family of low-molecular mass thermo-resistant proteins (6–8 kDa), with high cysteine content and a high affinity for various metals, especially for Ag ions. Following induction, MT responds quite easily via the metal responsive transcription factor (induced by triggers from the external environment) to generate changes in the intracellular metal distribution. The presence of AgNPs significantly changed the subcellular Ag distribution, with an increasing fraction of Ag associated with granules (fraction D), and a decreased fraction associated with fraction G (cytosol).

In the present study, the increase in CAT coincided with an increase in SOD when the worms were exposed to Ag⁺ (S AgNP) and Ag⁺ (L AgNP). This behavior might be related to the associated sequential changes in oxidative stress response by *E. fetida*: first, SOD converts O_2^- to H_2O_2, and then CAT converts H_2O_2 to H_2O, which indicates that SOD and CAT play a role in modulating reactive oxygen species whereas both are more sensitive to ionic Ag than to particulate Ag. Surprisingly, MDA concentrations resulting from lipid peroxidation were not increased in exposed worms. This probably results from the up-regulation of antioxidant defenses.

Metabolomics can perform a global analysis of the effects induced by AgNPs and the released Ag⁺. Due to the identical concentrations of Ag⁺ released from AgNPs at both sides of the semi-permeable membrane (Figure S3), the metabolomic analysis can provide a direct comparison of the metabolic responses to indicate the similarities and differences of effects induced by AgNP and Ag⁺ exposures. In both released Ag⁺ treatments, the two intermediates in the Krebs cycle, succinate and fumarate, were significantly elevated and depleted, respectively. Interestingly, succinate and fumarate levels were similarly altered in both S AgNP- and L AgNP-exposed groups, which demonstrated that the effects on these two intermediates in the Krebs cycle in *E. fetida* were induced by the released Ag⁺. In addition, increased alanine and phosphocholine levels were observed in S AgNP and Ag⁺ (S AgNP) treatments, but not in L AgNP and Ag⁺ (L AgNP) treatments. These two metabolic biomarkers probably indicated Ag⁺ concentration-dependent responses in *E. fetida* since the concentration of Ag⁺ (S AgNP) was approximately two times higher than the concentration of Ag⁺ (L AgNP) (Figure 3). Decreased levels of threonine, arginine and myo-inositol were seen in the Ag⁺ (S AgNP) treatment, but not in the S AgNP treatment, which suggests antagonistic effects between S AgNP and Ag⁺ (S AgNP). The unique metabolic responses, including decreased malate and glucose levels in S AgNP-treated *E. fetida* could be induced by S AgNP. Similarly, increased aspartate, asparagine and phenylalanine and decreased glucose and maltose levels were observed in the Ag⁺ (L AgNP)-treated group but not in the L AgNP treatment, which indicates

antagonistic interactions between L AgNP and Ag⁺ (L AgNP). Finally, the unique metabolic responses, including increased leucine, arginine and inosine, and decreased ATP levels in L AgNP-treated *E. fetida* samples are likely to be induced by L AgNP particles themselves.

The Krebs cycle intermediates, succinate and fumarate, were significantly ($p < 0.05$) increased and decreased in all AgNP and released Ag⁺-exposed earthworms, respectively. In the Krebs cycle, succinate can be converted into fumarate by succinate dehydrogenase (Lankadurai et al., 2013). The alteration of succinate and fumarate levels means a possible disruption in the conversion of succinate to fumarate induced by the released Ag⁺ (Lankadurai et al., 2011; Parrish et al., 1998). Since succinate dehydrogenase is the only enzyme bound to the inner mitochondrial membrane in the Krebs cycle, Ag⁺ released from AgNPs probably disrupts the functioning of succinate dehydrogenase by binding to the inner mitochondrial membrane and affecting its stabilization (Horton et al., 2006). A similar phenomenon was observed in phenanthrene-exposed *E. fetida* (Lankadurai et al., 2013). Alanine can be involved in the metabolic pathway of gluconeogenesis since it is the major substrate. The observed elevation of alanine levels in the S AgNP treatment indicated the inhibition of gluconeogenesis together with a decreased glucose level. Phosphocholine can be synthesized by conversion of ATP and choline into phosphocholine and ADP, catalyzed by choline kinase. Another intermediate in the Krebs cycle, malate, was depleted in the S AgNP-treated group, which implied disturbance of the Krebs cycle. Hence, these metabolic biomarkers clearly indicated the disruption of energy metabolism in S AgNP-treated earthworms induced by both S AgNP and its released Ag⁺. However, the decreased concentrations of the amino acids threonine and arginine suggest an enhanced protein synthesis in earthworms exposed to Ag⁺ (S AgNP), which was not observed in S AgNP-exposed animals. As an osmolyte, myo-inositol was decreased in the Ag⁺ (S AgNP)-exposed group, indicating a disruption of osmotic regulation by Ag⁺ (S AgNP).

Besides the possible disruption in the conversion of succinate to fumarate induced by the released Ag⁺ as indicated by the altered succinate and fumarate levels, the decreased ATP level implied an enhanced energy consumption in L AgNP-exposed earthworms, together with increased concentrations of the amino acids leucine and arginine, due to the breakdown of proteins (Bundy et al., 2002; Jones et al., 2008). Inosine is an intermediate in a chain of purine nucleotide reactions required for muscle movements. Therefore, the increase in inosine indicates the disturbance of muscle movements of *E. fetida* induced by L AgNP exposure. Maltose can be broken down to two molecules of glucose that are the substrates for glycolysis (Horton et al., 2006). Therefore, the decrease in maltose together with decreased glucose concentrations indicated an increasing energy requirement for Ag⁺ (L AgNP)-exposed earthworms. Previous studies showed that hydrophobic organic contaminants could result in an enhanced energy metabolism marked by decreased maltose and increased amino acid levels due to protein breakdown (Bundy et al., 2002; Jones et al., 2008). In our case, increased aspartate, asparagine and phenylalanine and decreased glucose and maltose levels were similarly observed in Ag⁺ (L AgNP)-exposed earthworms.

Conclusions

Two sizes of PVP-coated AgNPs were synthesized, and the Ag⁺ release of these two AgNPs was carefully determined by dialysis experiments using ICP-MS. Earthworms exposed for 96 h to the small and large AgNPs and the Ag⁺ ions released from these

particles, in simulated soil solutions, showed clear differences in Ag accumulation as well as in their biochemical responses. Although the uptake pathways and toxic effects of the AgNPs need more detailed studies, our data clearly show a different Ag subcellular partitioning pattern in the earthworms and also specific metabolite profiles caused by PVP-coated AgNPs compared with dissolved Ag (dissolution of Ag from the NPs). Besides similar alteration patterns identified in both the AgNP and the released Ag^+-treated groups, unique metabolic responses including decreased malate and glucose and increased leucine, arginine and inosine levels were observed in S AgNP-exposed *E. fetida*, together with decreased ATP in the L AgNP-exposed animals. These results add further evidence that AgNP toxicity cannot be completely attributed only to the dissolution of the AgNPs and release of Ag^+ ions.

Acknowledgements

Declaration of interest

References

Abei H. 1974. Catalase. In: Bergmeyer HU, ed. Methods of Enzymatic Analysis. New York: Academic Press, 673–84.

Bradford MM. 1976. A rapid and sensitive method for quantitation of microgram quantities of protein utilizing the principle of protein-dye binding. Anal Biochem 72:248–54.

Brown SAE, Simpson AJ, Simpson MJ. 2009. ^{1}H NMR metabolomics of earthworm responses to sub-lethal PAH exposure. Environ Chem 6: 432–40.

Bundy JG, Lenz EM, Bailey NJ, Gavaghan CL, Svendsen C, Spurgeon D, et al. 2002. Metabonomic assessment of toxicity of 4-fluoroaniline, 3,5-difluoroaniline and 2-fluoro-4-methylaniline to the earthworm *Eisenia veneta* (Rosa): identification of new endogenous biomarkers. Environ Toxicol Chem 21:1966–72.

Bundy JG, Spurgeon DJ, Svendsen C, Hankard PK, Weeks JM, Osborn D, et al. 2004. Environmental metabonomics: applying combination biomarker analysis in earthworms at a metal contaminated site. Ecotoxicology 13:797–806.

Cha KE, Myung H. 2007. Cytotoxic effects of nanoparticles assessed in vitro and in vivo. J Microbiol Biotechnol 17:1573–8.

Chae YJ, Chi PCH, Lee J, Bae E, Yi J, Gu MB. 2009. Evaluation of the toxic impact of silver nanoparticles on Japanese medaka (*Oryzias latipes*). Aquat Toxicol 94:320–7.

Cornelis G, Kirby JK, Beak D, Chittleborough D, McLaughlin MJ. 2010. A method for determination of retention of silver and cerium oxide manufactured nanoparticles in soils. Environ Chem 7:298–308.

Eom HJ, Choi J. 2010. p38 MAPK activation, DNA damage, cell cycle arrest and apoptosis as mechanisms of toxicity of silver nanoparticles in Jurkat T cells. Environ Sci Technol 44:8337–42.

García-Alonso J, Khan FR, Misra SK, Turmaine M, Smith BD, Rainbow PS, et al. 2011. Cellular internalization of silver nanoparticles in gut epithelia of the estuarine polychaete *Nereis diversicolor*. Environ Sci Technol 45:4630–6.

Guo Q, Sidhu JK, Ebbels TMD, Rana F, Spurgeon DJ, Svendsen C, et al. 2009. Validation of metabolomics for toxic mechanism of action screening with the earthworm *Lumbricus rubellus*. Metabolomics 5: 72–83.

He D, Bligh M, Waite TD. 2013. Effects of aggregate structure on the dissolution kinetics of citrate-stabilized silver nanoparticles. Environ Sci Technol 47:9148–56.

Horton HR, Moran LA, Scrimgeour KG, Perry MD, Rawn JD. 2006. Principles of Biochemistry. 4th ed. Upper Saddle River, NJ: Pearson Prentice Hall.

Ivask A, Elbadawy A, Kaweeteerawat C, Boren D, Fischer H, Ji Z, et al. 2014. Toxicity mechanisms in *Escherichia coli* vary for silver nanoparticles and differ from ionic silver. ACS Nano 28:374–86.

Jones OAH, Spurgeon DJ, Svendsen C, Griffin JL. 2008. A metabolomics based approach to assessing the toxicity of the polyaromatic hydrocarbon pyrene to the earthworm *Lumbricus rubellus*. Chemosphere 71: 601–9.

Kawata K, Osawa M, Okabe S. 2009. In vitro toxicity of silver nanoparticles at noncytotoxic doses to HepG2 human hepatoma cells. Environ Sci Technol 43:6046–51.

Kennedy A, Hull M, Bednar AJ, Goss J, Gunter J, Bouldin J, et al. 2010. Fractionating nanosilver: importance for determining toxicity to aquatic test organisms. Environ Sci Technol 44:9571–7.

Kiewiet AT, Ma WC. 1991. Effect of pH and calcium on lead and cadmium uptake by earthworms in water. Ecotoxicol Environ Saf 21: 32–7.

Kim J, Kim S, Lee S. 2011. Differentiation of the toxicities of silver nanoparticles and silver ions to the Japanese medaka (*Oryzias latipes*) and the cladoceran *Daphnia magna*. Nanotoxicol 5:208–14.

Kim S. 2009. Oxidative stress-dependent toxicity of silver nanoparticles in human hepatoma cells. Toxicol in Vitro 23:1076–84.

Kittler S, Greulich C, Diendorf J, Köller M, Epple M. 2010. Toxicity of silver nanoparticles increases during storage because of slow dissolution under release of silver ions. Chem Mater 22:4548–54.

Laban G, Nies LF, Turco RF, Bickham JW, Sepúlveda MS. 2010. The effects of silver nanoparticles on fathead minnow (*Pimephales promelas*) embryos. Ecotoxicol 19:185–95.

Lankadurai BP, Wolfe DM, Åslund MLW, Simpson AJ, Simpson MJ. 2013. ^{1}H NMR-based metabolomic analysis of polar and non-polar earthworm metabolites after sub-lethal exposure to phenanthrene. Metabolomics 9:44–56.

Lankadurai BP, Wolfe DM, Simpson AJ, Simpson MJ. 2011. ^{1}H NMR-based metabolomic analysis of the time dependent response of *Eisenia fetida* after sub-lethal phenanthrene exposure. Environ Pollut 159: 2845–51.

Li LZ, Zhou DM, Peijnenburg WJGM, van Gestel CAM, Jin SY, Wang YJ, et al. 2011. Toxicity of zinc oxide nanoparticles in the earthworm, *Eisenia fetida* and subcellular fractionation of Zn. Environ Int 37: 1098–104.

Liu JF, Chao JB, Liu R, Tan ZQ, Yin YG, Wu Y, et al. 2009. Cloud point extraction as an advantageous preconcentration approach for analysis of trace silver nanoparticles in environmental waters. Anal Chem 81: 6496–502.

Liu JY, Hurt RH. 2010. Ion release kinetics and particle persistence in aqueous nano-silver colloids. Environ Sci Technol 44:2169–75.

Luoma SN. 2008. Silver Nanotechnologies and the Environment: Old Problems or New Challenges? Washington, DC: Woodrow Wilson International Center for Scholars, Project on Emerging Nanotechnologies, and the PEW Charitable Trusts.

Meyer JN, Lord CA, Yang XYY, Turner EA, Badireddy AR, Marinakos SM, et al. 2010. Intracellular uptake and associated toxicity of silver nanoparticles in *Caenorhabditis elegans*. Aquat Toxicol 100: 140–50.

Miao AJ. 2009. The algal toxicity of silver engineered nanoparticles and detoxification by exopolymeric substances. Environ Pollut 157: 3034–41.

Mie G. 1908. A contribution to the optics of turbid media, especially colloidal metallic suspensions. Ann Phys 25:437–45.

Morones JR, Elechiguerra JL, Camacho A, Holt K, Kouri JB, Ramirez JT, et al. 2005. The bactericidal effect of silver nanoparticles. Nanotechnology 16:2346–53.

Mueller NC, Nowack B. 2008. Exposure modeling of engineered nanoparticles in the environment. Environ Sci Technol 42:4447–53.

Parrish AR, Alejandro NF, Bowes RC, Ramos KS. 1998. Cytotoxic response profiles of cultured renal epithelial and mesenchymal cells to selected aromatic hydrocarbons. Toxicology In Vitro 12:219–32.

Ratte H. 1999. Bioaccumulation and toxicity of silver compounds: a review. Environ Toxicol Chem 18:89–108.

Scanlan LD, Reed RB, Loguinov AV, Antczak P, Tagmount A, Aloni S, et al. 2013. Silver nanowire exposure results in internalization and toxicity to *Daphnia magna*. ACS Nano 23:10681–94.

Schnackenberg LK, Sun J, Beger RD. 2012. Metabolomics techniques in nanotoxicology studies. Methods Mol Biol 926:141–56.

Shoults-Wilson WA, Reinsch BC, Tsyusko OV, Bertsch PM, Lowry GV, Unrine JM. 2011a. Role of particle size and soil type in toxicity of silver nanoparticles to earthworms. Soil Sci Soc Am 75:365–77.

Shoults-Wilson WA, Reinsch BC, Tsyusko OV, Bertsch PM, Lowry GV, Unrine JM. 2011b. Effect of silver nanoparticle surface coating on bioaccumulation and reproductive toxicity in earthworms (*Eisenia fetida*). Nanotoxicol 5:432–44.

Shoults-Wilson WA, Zhurbich OI, McNear DH, Tsyusko OV, Bertsch PM, Unrine JM. 2011c. Evidence for avoidance of Ag nanoparticles by earthworms (*Eisenia fetida*). Ecotoxicology 20:385–96.

Sumner ME. 2000. Handbook of Soil Science. Boca Raton, FL: CRC Press Inc.

Tsyusko OV, Hardas SS, Shoults-Wilson WA, Starnes CP, Joice G, Butterfield DA, et al. 2012. Short-term molecular-level effects of silver nanoparticle exposure on the earthworm, *Eisenia fetida*. Environ Pollut 171:249–55.

Vijver MG, Van Gestel CAM, Lanno RP, Van Straalen NM, Peijnenburg WJGM. 2004. Internal metal sequestration and its ecotoxicological relevance: a review. Environ Sci Technol 38:4705–12.

Vijver MG, van Gestel CAM, van Straalen NM, Lanno RP, Peijnenburg WJGM. 2006. Biological significance of metals partitioned to subcellular fractions within earthworms (*Aporrectodeacaliginosa*). Environ Toxicol Chem 25:807–14.

Xiu ZM, Ma J, Alvarez PJ. 2011. Differential effect of common ligands and molecular oxygen on antimicrobial activity of silver nanoparticles versus silver ions. Environ Sci Technol 45:9003–8.

Yang X, Gondikas AP, Marinakos SM, Auffan M, Liu J, Hsu-Kim H, et al. 2012. Mechanism of silver nanoparticle toxicity is dependent on dissolved silver and surface coating in *Caenorhabditis elegans*. Environ Sci Technol 46:1119–27.

Yin L, Cheng Y, Espinasse B, Colman BP, Auffan M, Wiesner M, et al. 2011. More than the ions: the effects of silver nanoparticles on *lolium multiflorum*. Environ Sci Technol 45:2360–7.

Supplementary material available online
Supplementary Table S1 and Figures S1–S3.